ABC (Adventures in Bifurcations and Chaos) : A Program for Studying Chaos

by MICHAEL P. KENNEDY

Department of Electronic and Electrical Engineering, University College Dublin, Dublin 4, Ireland

ABSTRACT: *"Adventures in Bifurcations and Chaos" (ABC) is a user-friendly program for IBM-compatible PCs which has been designed for exploring bifurcations and chaos in the Chua oscillator paradigm. ABC calculates and draws equilibrium points, eigenvalues, eigenspaces, and trajectories. A two-dimensional projection of the three-dimensional dynamics is shown in a state space plot while the corresponding time waveforms are simultaneously displayed in a time-domain window. The software includes an extensive database of sets of initial conditions and parameters which produce many dynamical behaviors which have been reported for Chua's oscillator: equilibrium points, bifurcation sequences, periodic orbits, homoclinic and heteroclinic orbits and a plethora of chaotic attractors.*

I. Introduction

"Adventures in Bifurcations and Chaos" (ABC) is a user-friendly program for IBM-compatible PCs which has been designed for exploring bifurcations and chaos in the Chua oscillator paradigm. The program is written in Microsoft QuickBASIC and runs without compilation on any IBM-compatible PC with EGA or VGA graphics and version 5.0 or later of the Microsoft DOS operating system. ABC calculates and draws equilibrium points, eigenvalues, eigenspaces, and trajectories. A two-dimensional projection of the three-dimensional dynamics is shown in a state space plot while the corresponding time waveforms are simultaneously displayed in a time-domain window. The user may change the parameters, initial condition, and viewing angle. The ability to view the attractor in a variety of orientations and thus to "walk through" the three-dimensional state space permits one to visualize readily the geometric structure of the dynamics.

The software includes an extensive database of sets of initial conditions and parameters which produce many dynamical behaviors which have been reported for Chua's oscillator: equilibrium points, bifurcation sequences, periodic orbits, homoclinic and heteroclinic orbits, and a plethora of chaotic attractors.

II. The Chua Oscillator Paradigm

One of the simplest and most widely studied real nonlinear dynamical systems which produces complex steady-state behavior is Chua's oscillator (1), shown in
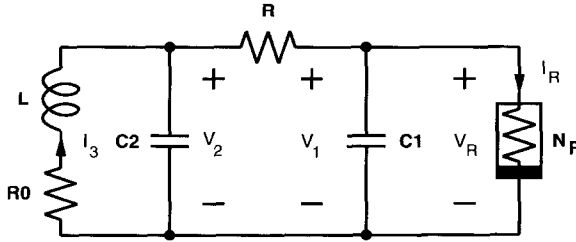
FIG. 1. Chua's oscillator consists of a linear inductor L with series resistance R_0, a linear resistor R, two linear capacitors C_1 and C_2, and a voltage-controlled nonlinear resistor N_R.

Fig. 1. This circuit consists of a linear inductor L in series with a linear resistor R_0†, a linear resistor R, two linear capacitors C_1 and C_2, and a single voltage-controlled‡ nonlinear resistor N_R called a *Chua diode* (**4**).

The driving-point (DP) characteristic of the Chua diode (shown in Fig. 2) has the form

$$I_R = f(V_R)$$
$$= G_b V_R + \tfrac{1}{2}(G_a - G_b)\{|V_R + E| - |V_R - E|\}$$
$$= \begin{cases} G_b V_R + (G_b - G_a)E & \text{if} \quad V_R < -E \\ G_a V_R & \text{if} \quad -E \leqslant V_R \leqslant E \\ G_b V_R + (G_a - G_b)E & \text{if} \quad V_R > E. \end{cases} \tag{1}$$

Chua's oscillator is readily constructed at low cost using standard electronic components (**4**) and exhibits a rich variety of bifurcations and chaos. Furthermore, this remarkable circuit is the first *physical* system, whose theoretical behavior agrees with both computer simulations and experimental results, for which the presence of chaos (in the sense of Shil'nikov) has been proven mathematically (**2**).

Just as the familiar parallel RLC resonant circuit is the simplest physical system
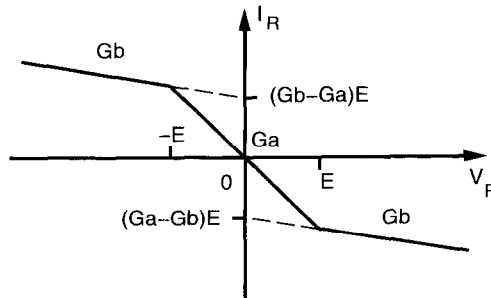

FIG. 2. The driving-point characteristic of the nonlinear resistor N_R in Chua's oscillator has breakpoints at $\pm E$ and slopes G_a and G_b in the inner and outer regions, respectively.

† When $R_0 = 0$, Chua's oscillator reduces to the original Chua's circuit (**2**).

‡ A two-terminal nonlinear resistor is called *voltage-controlled* if the current into its terminals may be written as a function of the voltage across it (**3**).

which can model the onset of oscillation in a dynamical system, so Chua's oscillator is the simplest paradigm for studying nonperiodic phenomena in nonlinear circuits (**5, 6**).

The ABC software package (**6**) has been developed to enable the user to explore the exciting world of bifurcations and chaos in the Chua's oscillator paradigm (**7**). Using this program, one may examine in detail the geometric structure, bifurcations, and periodic and nonperiodic oscillatory phenomena in Chua's oscillator.

In the following sections, we analyze the dynamical behavior of Chua's oscillator, give a tutorial introduction to bifurcations and chaos using the ABC program, and illustrate by example many of the characteristic steady-state solutions of the oscillator.

2.1. *State equations*

Chua's oscillator is described by a set of three ordinary differential equations called Chua's equations:

$$\frac{dI_3}{dt} = -\frac{R_0}{L}I_3 - \frac{1}{L}V_2 \tag{2}$$

$$\frac{dV_2}{dt} = \frac{1}{C_2}I_3 - \frac{G}{C_2}(V_2 - V_1) \tag{3}$$

$$\frac{dV_1}{dt} = \frac{G}{C_1}(V_2 - V_1) - \frac{1}{C_1}f(V_1)$$

$$= \begin{cases} \dfrac{G}{C_1}V_2 - \dfrac{G_b'}{C_1}V_1 - \left(\dfrac{G_b - G_a}{C_1}\right)E & \text{if} \quad V_1 < -E \\[3mm] \dfrac{G}{C_1}V_2 - \dfrac{G_a'}{C_1}V_1 & \text{if} \quad -E \leqslant V_1 \leqslant E \\[3mm] \dfrac{G}{C_1}V_2 - \dfrac{G_b'}{C_1}V_1 - \left(\dfrac{G_a - G_b}{C_1}\right)E & \text{if} \quad V_1 > E \end{cases} \tag{4}$$

where $G = 1/R$, $G_a' = G + G_a$, and $G_b' = G + G_b$. This is an autonomous dynamical system of the form

$$\frac{dX(t)}{dt} = F(X(t))$$

where $X(t) = [I_3(t), V_2(t), V_1(t)]^T$ is called the *state* of the system at time t. A solution $X(t)$ starting from an initial state $[I_3(0), V_2(0), V_1(0)]^T$ is called a *trajectory* of Chua's oscillator.

Because of the piecewise-linear nature of the Chua diode DP characteristic, the state space is partitioned by the boundary planes U_{-1} ($V_1 \equiv -E$) and U_1 ($V_1 \equiv E$) into three distinct regions: D_0 ($-E \leqslant V_1 \leqslant E$), D_{-1} (where $V_1 < -E$), and D_1 (where $V_1 > E$). We can consider separately the dynamical behavior in each of these regions.
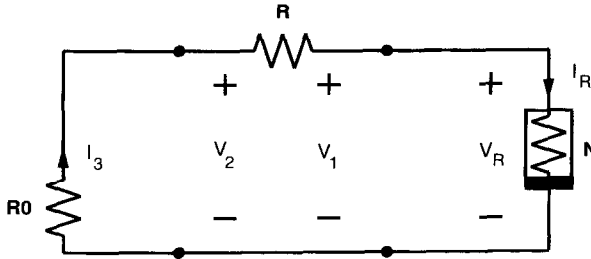
FIG. 3. DC equivalent circuit of Fig. 1 obtained by short-circuiting the inductor L and open-circuiting capacitors C_1 and C_2.

2.2. *Equilibrium points*

The equilibrium points of Chua's oscillator are defined by

$$0 = -\frac{R_0}{L}I_3 - \frac{1}{L}V_2$$

$$0 = \frac{1}{C_2}I_3 - \frac{G}{C_2}(V_2 - V_1)$$

$$0 = \frac{G}{C_1}(V_2 - V_1) - \frac{1}{C_1}I_R$$

where I_R is given by Eq. (1). An equilibrium point is simply a solution of the DC equivalent circuit which is obtained by short-circuiting L and open-circuiting C_1 and C_2 (3), as shown in Fig. 3.

The solution of this circuit is $I_R = -G'V_R$, where $G' = 1/(R+R_0) = G/(1+GR_0)$. The equilibrium points may be determined graphically by intersecting the *load line* $I_R = -G'V_R$ with the DP characteristic $I_R = f(V_R)$ of the nonlinear resistor N_R, as shown in Fig. 4 (3). Note that the circuit *always* has an equilibrium point (denoted **0**) in the D_0 region.

The points $\mathbf{P}_-$ and $\mathbf{P}_+$ associated with the outer regions D_{-1} and D_1 are defined by $V_1 = -I'/(G_b+G')$, $V_2 = (R_0/(R_0+R))V_1$, and $I_3 = -G'V_1$, where $I' = (G_b - G_a)E$ in D_{-1} and $I' = (G_a - G_b)E$ in D_1 (see Fig. 2).

FIG. 4. DC equilibrium points of Fig. 1 may be determined graphically by intersecting the load line $I_R = -GV_R$ with the DP characteristic of N_R. (a) If $G' > |G_a|$ or $G' < |G_b|$, the circuit has a unique equilibrium point at the origin ($\mathbf{P}_-$ and $\mathbf{P}_+$ are *virtual equilibria* in this case). (b) When $|G_b| < G' < |G_a|$, the circuit has three equilibrium points at $\mathbf{P}_-$, $\mathbf{O}$, and $\mathbf{P}_+$.

Thus,

$$
\mathbf{P}_- = \begin{bmatrix} \dfrac{G(G_b - G_a)}{G'_b + GG_b R_0} E \\[2ex] -\dfrac{GR_0(G_b - G_a)}{G'_b + GG_b R_0} E \\[2ex] -\dfrac{(1 + GR_0)(G_b - G_a)}{G'_b + GG_b R_0} E \end{bmatrix}, \quad \mathbf{P}_+ = \begin{bmatrix} \dfrac{G(G_a - G_b)}{G'_b + GG_b R_0} E \\[2ex] -\dfrac{GR_0(G_a - G_b)}{G'_b + GG_b R_0} E \\[2ex] -\dfrac{(1 + GR_0)(G_a - G_b)}{G'_b + GG_b R_0} E \end{bmatrix}. \quad (5)
$$

If $\mathbf{P}_-$ lies *inside* the D_{-1} region, then it is an equilibrium point of Chua's oscillator. If $\mathbf{P}_-$ lies *outside* the D_{-1} region, then it is called a *virtual* equilibrium point (3). Note that the equilibrium point $\mathbf{P}_-$ lies *outside* D_{-1} (and so is a virtual equilibrium point) if

$$
-\frac{(1 + GR_0)(G_b - G_a)}{G'_b + GG_b R_0} E > -E.
$$

In summary, if $G' > |G_a|$ or $G' < |G_b|$, the circuit has a unique equilibrium point at the origin and two virtual equilibria $\mathbf{P}_-$ and $\mathbf{P}_+$; otherwise, it has three equilibrium points at $\mathbf{P}_-$, $\mathbf{0}$, and $\mathbf{P}_+$.†

2.3. Dynamics of the inner and outer regions

Associated with each of the points $\mathbf{P}_-$, $\mathbf{0}$, and $\mathbf{P}_+$ are three eigenvalues which determine the dynamics in the D_{-1}, D_0, and D_1 regions, respectively.

2.3.1. *The D_0 region*. When $|V_1| \leqslant E$, Chua's oscillator is described by

$$
\frac{dI_3}{dt} = -\frac{R_0}{L} I_3 - \frac{1}{L} V_2
$$

$$
\frac{dV_2}{dt} = \frac{1}{C_2} I_3 - \frac{G}{C_2}(V_2 - V_1)
$$

$$
\frac{dV_1}{dt} = \frac{G}{C_1} V_2 - \frac{G'_a}{C_1} V_1.
$$

The circuit has an equilibrium point at the origin whose stability is completely specified by the eigenvalues of

$$
\mathbf{J}_{\mathbf{Fa}} = \begin{bmatrix} -\dfrac{R_0}{L} & -\dfrac{1}{L} & 0 \\[2ex] \dfrac{1}{C_2} & -\dfrac{G}{C_2} & \dfrac{G}{C_2} \\[2ex] 0 & \dfrac{G}{C_1} & -\dfrac{G'_a}{C_1} \end{bmatrix},
$$

namely the zeros of the characteristic polynomial

†We exclude the cases when there are infinitely many equilibrium points, i.e. when $G' \equiv -G_a$.

$$\lambda^3 + \left(\frac{G}{C_2} + \frac{G_a'}{C_1} + \frac{R_0}{L}\right)\lambda^2 + \left(\frac{1 + GR_0}{LC_2} + \frac{G_a'R_0}{LC_1} + \frac{GG_a}{C_1 C_2}\right)\lambda + \frac{GG_a R_0 + G_a'}{LC_1 C_2}. \quad (6)$$

Throughout this paper, we consider a fixed set of component values: $L = 18$ mH, $C_2 = 100$ nF, $C_1 = 10$ nF, $R_0 = 12.5\ \Omega$, $G_a = -50/66$ mS $= -757.576\ \mu$S, $G_b = -9/22$ mS $= -409.09\ \mu$S, and $E = 1$ V.

When $G = 550\ \mu$S, the eigenvalues of $\mathbf{J_{Fa}}$ are:

$$\gamma_0 \approx 26527$$

$$\sigma_0 \pm j\omega_0 \approx -5982 \pm j20200.$$

Associated with the unstable real eigenvalue γ_0 in the D_0 region is an eigenvector $E^r(\mathbf{0})$ which is defined by

$$\mathbf{J_{Fa}} E^r(\mathbf{0}) = \gamma_0 E^r(\mathbf{0}).$$

Writing $E^r(\mathbf{0}) = [x, y, z]^T$, we have

$$\begin{bmatrix} \gamma_0 + \dfrac{R_0}{L} & \dfrac{1}{L} & 0 \\[2mm] -\dfrac{1}{C_2} & \gamma_0 + \dfrac{G}{C_2} & -\dfrac{G}{C_2} \\[2mm] 0 & -\dfrac{G}{C_1} & \gamma_0 + \dfrac{G_a'}{C_1} \end{bmatrix} \begin{bmatrix} x \\ y \\ z \end{bmatrix} = \begin{bmatrix} 0 \\ 0 \\ 0 \end{bmatrix}.$$

Normalized to $z = 1$, the corresponding eigenvector is:

$$E^r(\mathbf{0}) = \begin{bmatrix} x \\ y \\ z \end{bmatrix} = \begin{bmatrix} \left(\gamma_0 + \dfrac{G}{C_2}\right)\left(\gamma_0 + \dfrac{G_a'}{C_1}\right)\dfrac{C_1 C_2}{G} - G \\[4mm] \dfrac{C_1}{G}\left(\gamma_0 + \dfrac{G_a'}{C_1}\right) \\[4mm] 1 \end{bmatrix}. \quad (7)$$

The real and imaginary parts of the complex eigenvectors associated with $\sigma_0 \pm j\omega_0$ span a *complex eigenplane* which we denote by $E^c(\mathbf{0})$. The vector $\mathbf{n}_{E^c(\mathbf{0})}$ normal to $E^c(\mathbf{0})$ has the property that

$$(\mathbf{X} - \mathbf{0}) \cdot \mathbf{n}_{E^c(\mathbf{0})} = 0, \forall\, \mathbf{X} \in E^c(\mathbf{0}).$$

Thus,

$$\mathbf{n}_{E^c(\mathbf{0})} = \begin{bmatrix} -\dfrac{LC_2}{G}\left(\gamma_0 + \dfrac{G_a'}{C_1}\right)\left(\gamma_0 + \dfrac{G}{C_2}\right) + \dfrac{LG}{C_1} \\[4mm] \dfrac{C_2}{G}\left(\gamma_0 + \dfrac{G_a'}{C_1}\right) \\[4mm] 1 \end{bmatrix} = \begin{bmatrix} -\dfrac{L}{C_1}x \\[4mm] \dfrac{C_2}{C_1}y \\[4mm] z \end{bmatrix}, \quad (8)$$

where γ_0 is the *real* eigenvalue in D_0.

This plane is characterized by the fact that for every $\mathbf{X} \in E^c(\mathbf{0})$, $\mathbf{J}_{Fa}\mathbf{X} \in E^c(\mathbf{0})$. Thus, a trajectory starting on the eigenplane $E^c(\mathbf{0})$ evolves along $E^c(\mathbf{0})$, and a trajectory cannot cross through an eigenplane. An important consequence of this is that a trajectory which originates from an initial state above the eigenplane remains indefinitely above the plane, and one which originates below $E^c(\mathbf{0})$ remains forever below the plane.

We have the following qualitative description of the D_0 dynamics. A trajectory starting from some initial state $\mathbf{X}_0$ in the D_0 region may be decomposed into its components along the complex eigenplane $E^c(\mathbf{0})$ and along the eigenvector $E^r(\mathbf{0})$. When $\gamma_0 > 0$ and $\sigma_0 < 0$, the component along $E^c(\mathbf{0})$ spirals towards the origin along this plane while the component in the direction $E^r(\mathbf{0})$ grows exponentially. Adding the two components, we see that a trajectory starting slightly above the stable complex eigenplane $E^c(\mathbf{0})$ spirals towards the origin along the $E^c(\mathbf{0})$ direction, all the while being pushed away from $E^r(\mathbf{0})$ along the unstable direction $E^r(\mathbf{0})$. As the (stable) component along $E^c(\mathbf{0})$ shrinks in magnitude, the (unstable) component grows exponentially, and the trajectory follows a helix of exponentially decreasing radius whose axis lies in the direction of $E^r(\mathbf{0})$; this is illustrated in Fig. 5.

2.3.2. *The D_{-1} and D_1 regions.* In the outer regions ($|V_1| > E$), Chua's oscillator (with a piecewise-linear N_R) is described by

$$\frac{dI_3}{dt} = -\frac{R_0}{L} - \frac{1}{L}V_2$$

$$\frac{dV_2}{dt} = \frac{1}{C_2}I_3 - \frac{G}{C_2}(V_2 - V_1)$$

$$\frac{dV_1}{dt} = \frac{G}{C_1}V_2 - \frac{G_b'}{C_1}V_1 - \frac{I'}{C_1}$$
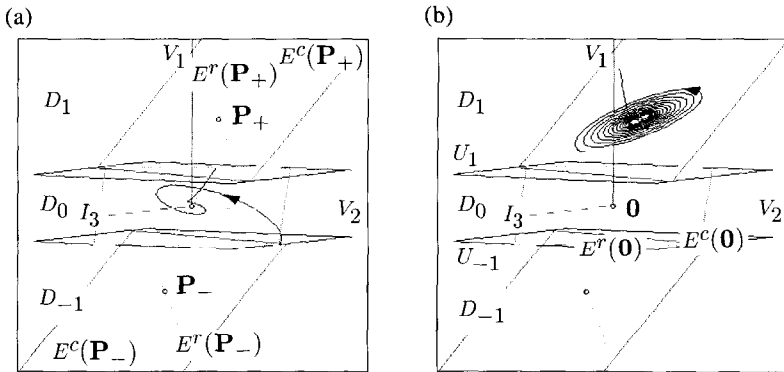
(a)

(b)

FIG. 5. (a) Dynamics of the D_0 region. A trajectory starting slightly above the stable complex eigenplane $E^c(\mathbf{0})$ spirals towards the origin along this plane and is repelled close to $\mathbf{0}$ in the direction of the unstable eigenvector $E^r(\mathbf{0})$. (b) Dynamics of the D_1 region. A trajectory starting above the unstable complex eigenplane $E^c(\mathbf{P}_+)$ close to the eigenvector $E^r(\mathbf{P}_+)$ moves towards the plane and spirals away from $\mathbf{P}_+$ along $E^c(\mathbf{P}_+)$. By symmetry, the D_{-1} region has equivalent dynamics.

where $I' = (G_b - G_a)E$ when $V_1 < -E$ (the D_{-1} region), and $I' = (G_a - G_b)E$ when $V_1 > E$ (the D_1 region).

We can determine the stability of the equilibrium points ($\mathbf{P}_-$ and $\mathbf{P}_+$) and the dynamics of the outer regions by examining the Jacobian matrix

$$
\mathbf{J_{Fb}} = \begin{bmatrix} -\dfrac{R_0}{L} & -\dfrac{1}{L} & 0 \\[2mm] \dfrac{1}{C_2} & -\dfrac{G}{C_2} & \dfrac{G}{C_2} \\[2mm] 0 & \dfrac{G}{C_1} & -\dfrac{G'_b}{C_1} \end{bmatrix},
$$

whose eigenvalues are the zeroes of the characteristic polynomial

$$
\lambda^3 + \left(\frac{G}{C_2} + \frac{G'_b}{C_1} + \frac{R_0}{L} \right)\lambda^2 + \left(\frac{1 + GR_0}{LC_2} + \frac{G'_b R_0}{LC_1} + \frac{GG_b}{C_1 C_2} \right)\lambda + \frac{GG_b R_0 + G'_b}{LC_1 C_2}. \quad (9)
$$

With all other component values as before, and $G = 550\ \mu\text{S}$, the eigenvalues of $\mathbf{J_{Fb}}$ are:

$$
\gamma_1 \approx -21158
$$

$$
\sigma_1 \pm j\omega_1 \approx 436 \pm j19000.
$$

Associated with the unstable real eigenvalue γ_1 in the D_1 region is an eigenvector $E^r(\mathbf{P}_+)$ which is defined by

$$
\mathbf{J_{Fb}} E^r(\mathbf{P}_+) = \gamma_1 E^r(\mathbf{P}_+).
$$

Writing $E^r(\mathbf{P}_+) = [x, y, z]^T$, we have

$$
\begin{bmatrix} \gamma_1 + \dfrac{R_0}{L} & \dfrac{1}{L} & 0 \\[2mm] -\dfrac{1}{C_2} & \gamma_1 + \dfrac{G}{C_2} & -\dfrac{G}{C_2} \\[2mm] 0 & -\dfrac{G}{C_1} & \gamma_1 + \dfrac{G'_b}{C_1} \end{bmatrix} \begin{bmatrix} x \\ y \\ z \end{bmatrix} = \begin{bmatrix} 0 \\ 0 \\ 0 \end{bmatrix}.
$$

Normalized to $z = 1$, the real eigenvector is:

$$
E^r(\mathbf{P}_+) = \begin{bmatrix} x \\ y \\ z \end{bmatrix} = \begin{bmatrix} \left(\gamma_1 + \dfrac{G}{C_2}\right)\left(\gamma_1 + \dfrac{G'_b}{C_1}\right)\dfrac{C_1 C_2}{G} - G \\[3mm] \dfrac{C_1}{G}\left(\gamma_1 + \dfrac{G'_b}{C_1}\right) \\[3mm] 1 \end{bmatrix}. \quad (10)
$$

The real and imaginary parts of the complex eigenvectors associated with $\sigma_1 \pm j\omega_1$ span a complex eigenplane which we denote $E^c(\mathbf{P}_+)$.

The vector $\mathbf{n}_{E^c(\mathbf{P}_+)}$ normal to $E^c(\mathbf{P}_+)$ has the property that

$$(\mathbf{X} - \mathbf{P}_+) \cdot \mathbf{n}_{E^c(\mathbf{P}_+)} = 0, \forall \mathbf{X} \in E^c(\mathbf{P}_+).$$

Thus,

$$\mathbf{n}_{E^c(\mathbf{P}_+)} = \begin{bmatrix} -\dfrac{LC_2}{G}\left(\gamma_1 + \dfrac{G_b'}{C_1}\right)\left(\gamma_1 + \dfrac{G}{C_2}\right) + \dfrac{LG}{C_1} \\[6pt] \dfrac{C_2}{G}\left(\gamma_1 + \dfrac{G_b'}{C_1}\right) \\[6pt] 1 \end{bmatrix} = \begin{bmatrix} -\dfrac{L}{C_1}x \\[6pt] \dfrac{C_2}{C_1}y \\[6pt] z \end{bmatrix}, \tag{11}$$

where γ_1 is the *real* eigenvalue in D_1.

This eigenplane is characterized by the fact that for every $\mathbf{X} \in E^c(\mathbf{P}_+)$, $\mathbf{J}_{\mathrm{Fb}}\mathbf{X} \in E^c(\mathbf{P}_+)$, so a trajectory starting on $E^c(\mathbf{P}_+)$ evolves along $E^c(\mathbf{P}_+)$. Once again, we note that a trajectory which originates from an initial state above the complex eigenplane remains indefinitely above the plane, and one which originates below remains below.

We have the following qualitative description of the D_1 dynamics. Associated with the stable real eigenvalue γ_1 in the D_1 region is the eigenvector $E^r(\mathbf{P}_+)$. The real and imaginary parts of the complex eigenvectors associated with $\sigma_1 \pm j\omega_1$ define a complex eigenplane $E^c(\mathbf{P}_+)$.

A trajectory starting from some initial state $\mathbf{X}_0$ in the D_1 region may be decomposed into its components along the complex eigenplane $E^c(\mathbf{P}_+)$ and the eigenvector $E^r(\mathbf{P}_+)$. When $\gamma_1 < 0$ and $\sigma_1 > 0$, the component on $E^c(\mathbf{P}_+)$ spirals away from $\mathbf{P}_+$ along this plane while the component in the direction of $E^r(\mathbf{0})$ tends asymptotically towards $\mathbf{P}_+$. Adding the two components, we see that a trajectory starting close to the stable real eigenvector $E^r(\mathbf{P}_+)$ above the complex eigenplane moves towards $E^c(\mathbf{P}_+)$ along a helix of exponentially increasing radius. Since the component along $E^r(\mathbf{P}_+)$ shrinks exponentially in magnitude and the component on $E^c(\mathbf{P}_+)$ grows exponentially, the trajectory is quickly flattened onto $E^c(\mathbf{P}_+)$, where it spirals away from $\mathbf{P}_+$ along the complex eigenplane; this is illustrated in Fig. 5(b).

Note that because of the strong rate of contraction along the $E^r(\mathbf{P}_+)$ direction, a trajectory spends most of its time in D_1 coasting very close to $E^c(\mathbf{P}_+)$. Consequently, the system appears locally to be two-dimensional and can therefore be readily analyzed using one-dimensional discrete maps [see (8) for example].

By symmetry, the equilibrium point $\mathbf{P}_-$ in the D_{-1} region has three eigenvalues, namely γ_1 and $\sigma_1 \pm j\omega_1$. The eigenvector $E^r(\mathbf{P}_-)$ is associated with the stable real eigenvalue γ_1; the real and imaginary parts of the eigenvectors associated with the unstable complex pair $\sigma_1 \pm j\omega_1$ define an eigenplane $E^c(\mathbf{P}_-)$ along which trajectories spiral away from $\mathbf{P}_-$.

III. Algorithm

ABC enables one to study the evolution of trajectories in Chua's oscillator by solving Chua's equations numerically.

The user sets the parameters of Chua's oscillator and the initial values of the state variables. The parameters define the geometry of the phase space and the initial values define the start of a particular trajectory.

Using Eq. (5), ABC first calculates the positions of the points $\mathbf{P}_-$, $\mathbf{0}$, and $\mathbf{P}_+$. The eigenvalues of the inner and outer regions are then determined by solving the characteristic polynomials (6) and (9), respectively, using Cardano's method (9). These are printed in a box on the right-hand side of the screen. ABC also determines the magnitude of the largest eigenvalue $|\lambda_{\max}|$ of the system.

The eigenspaces $E^r(\mathbf{P}_+)$, $E^c(\mathbf{P}_+)$, $E^r(\mathbf{0})$, $E^c(\mathbf{0})$, $E^r(\mathbf{P}_-)$, and $E^c(\mathbf{P}_-)$ are constructed using the appropriate eigenvectors and normal vectors defined by Eqs (7), (8), (10), and (11)†.

From a user-specified initial state, a solution trajectory is calculated by numerically integrating Chua's equations using a fourth-order Runge–Kutta integration routine (10) with a fixed timestep h for a selected number N of time points. The default values for the timestep and number of points are $0.25/|\lambda_{\max}|$ and 1024, respectively.

The state $\mathbf{X}(t+h)$ at time $t+h$ is determined from the state $\mathbf{X}(t)$ at time t in five steps:

$$\mathbf{K_1} = h\mathbf{F}(\mathbf{X}(t))$$

$$\mathbf{K_2} = h\mathbf{F}(\mathbf{X}(t)+\tfrac{1}{2}\mathbf{K_1})$$

$$\mathbf{K_3} = h\mathbf{F}(\mathbf{X}(t)+\tfrac{1}{2}\mathbf{K_2})$$

$$\mathbf{K_4} = h\mathbf{F}(\mathbf{X}(t)+\mathbf{K_3})$$

$$\mathbf{X}(t+h) = \mathbf{X}(t)+\tfrac{1}{6}\mathbf{K_1}+\tfrac{1}{3}\mathbf{K_2}+\tfrac{1}{3}\mathbf{K_3}+\tfrac{1}{6}\mathbf{K_4}.$$

The waveforms $I_3(t)$, $V_2(t)$, and $V_1(t)$ are displayed in a "time window" at the top of the screen. The state space trajectory $[I_3, V_2, V_1]^T$ is simultaneously plotted in a "phase window".

The (I_3, V_2, V_1) coordinate system in state space may be rotated under user control to any desired orientation so that the trajectory may be viewed from a user-specified angle.

IV. ABC Tutorial

ABC is supplied as QuickBasic source code (ABC.BAS) and in executable form (ABC.EXE). The executable version ABC.EXE may be run by typing abc.

The source code ABC.BAS may be edited and run using the QuickBasic interpreter, supplied with DOS 5.0, by typing qbasic abc. When the blue screen of

†If the oscillator has three *real* eigenvectors λ_1, λ_2, and λ_3 in any region, ABC draws the eigenvector corresponding to λ_1 and the eigenplane spanned by the eigenvectors of λ_2 and λ_3.

```
CHUA OSCILLATOR

t   ■ 250  µs/div
I3      1 mA/div
U2    200 mV/div
V1  ■   1  V/div
```

```
      PARAMETER
L    +  18.000 mH
R0   +  12.500  Ω
C2   +100.000 nF
G    +565.000 µS
Ga   -757.576 µS
Gb   -409.090 µS
E    +   1.000  V
C1   +  10.000 nF
```

```
   CURRENT STATE
I3   +   2.734 mA
V2   +250.071 mV
V1   -   2.800  V
```

```
∅  86°   ESPACES
θ  30°     ON
```

```
    EIGENVALUES

OUTER  REGION
 -2.3148D+04,
 +6.0645D+02
+/-j0.192D+05

INNER  REGION
 +2.5358D+04,
 -6.2222D+03
+/-j0.199D+05
```

```
OPTIONS   FILE


DATA FILE  (C)
```

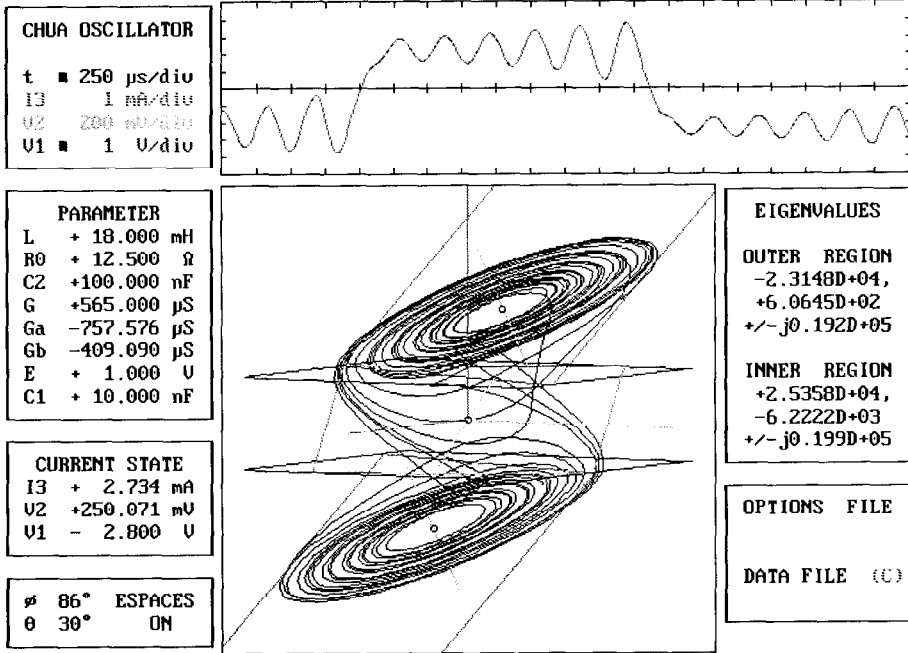`<A>xes <B>uffer <C>lr <F>ile <I>ntegration <P>arams <Q>uit <R>un <S>tate <V>iew`

FIG. 6. ABC screen, showing dialog boxes, message box, "time window" and "phase window". The "phase window" shows a view of a Double Scroll Chua's attractor. Note that $V_1(t)$ is displayed in the "time window".

the QuickBasic environment appears, press ⌐Shift F5⌐ (⌐Shift⌐ and ⌐F5⌐ simultaneously)† to run ABC. The const MAXTIMESERIESLENGTH may be decreased if an "out of memory" error occurs.

Once ABC is running, eight boxes and a Help message appear on the screen, as shown in Fig. 6. These are: the Axes dialog box‡, the Parameter dialog box, the State dialog box, the View dialog box, the "time window", the "phase window", the Eigenvalues message box, and the File dialog box.

The main menu shown on the Help line consists of the choices ⟨A⟩xes, ⟨B⟩uffer, ⟨C⟩lr, ⟨F⟩ile, ⟨I⟩ntegration, ⟨P⟩arams, ⟨Q⟩uit, ⟨R⟩un, ⟨S⟩tate, and ⟨V⟩iew. Each choice can be selected by typing the first letter of the appropriate word. For example, typing ⌐F⌐ will enter the ⟨F⟩ile submenu. Within each submenu, the main menu can be reached by hitting the ⌐Esc⌐ (Escape) key, and the previous menu can be reached by hitting the ⌐CR⌐ (Carriage Return) key.

4.1. *Dialog boxes*

4.1.1. *Axes.* The Axes dialog box shows the scaling factors used for displaying the state variables.

†In this manual, we denote keystrokes by boxed letters. Thus, ⌐D⌐ denotes the key labelled D.

‡A *dialog* box is one through which the user may provide input for the program.

```
┌─────────────────────────┐
│   CHUA OSCILLATOR       │
│                         │
│  t    ■   250   µs/div  │
│                         │
│  I3   ■     1   mA/div  │
│                         │
│  V2   ■   200   mV/div  │
│                         │
│  V1   ■     1   V/div   │
└─────────────────────────┘
```

FIG. 7. Axes dialog box.

```
┌─────────────────────────┐
│    CURRENT STATE        │
│                         │
│  I3   +    1.805   mA   │
│                         │
│  V2   +  166.006   mV   │
│                         │
│  V1   -    2.359   V    │
└─────────────────────────┘
```

FIG. 8. State dialog box.

The time axis of the "time window" (to the right of the Axes dialog box) is subdivided into twenty divisions at 250 µs/div. The vertical axis of the "time window" is subdivided into 10 divisions.

The squares indicate that the corresponding variables will be displayed in the "time window". For example, if the I3 square is not showing, $I_3(t)$ will not be drawn.

To modify the values in the Axes box, type A at the main menu. A flashing cursor appears in the Axes box. The values can then be changed by moving the cursor with the arrow keys and either incrementing or decrementing the current value by means of the + and − keys, or by entering the digits directly from the keyboard.

Pressing A in the Axes submenu will change the scales to fit the trajectory in the time window and phase window. By hitting the K key, the value of the axis where the cursor currently resides can be entered by typing the value on the bottom of the screen and hitting CR . In this case, Backspace can be used to edit the value before hitting CR . See Fig. 7.

Exponents can also be used when entering values from the keyboard. This feature is useful when entering data with high precision as the dialog box only prints out a small number of significant digits.

4.1.2. State. The State dialog box shows the current values of the state variables I_3, V_2, and V_1. Select the State dialog window by pressing the S key. See Fig. 8.

Each state variable may be initialized by moving the cursor with the arrow keys and either incrementing or decrementing the current value by means of the + and − keys, or entering directly from the keyboard the values of the appropriate digits. One may also enter default values for the state vector by pressing the D key. By pressing the K key, values can be entered from the keyboard in the same way as for the Axes box.

4.1.3. Parameter. The Parameter dialog box displays the values of the parameters

```
        PARAMETER

L    +     18.000   mH

RO   +     12.500   Ω

C2   +    100.000   nF

G    +    565.000   μS

Ga   -    757.576   μS

Gb   -    409.090   μS

E    +      1.000   V

C1   +     10.000   nF
```

FIG. 9. Parameter dialog box.

of Chua's oscillator. The default values (for a Double Scroll Chua's attractor) are shown in Fig. 9.

The next step in running a simulation of Chua's oscillator is to set the values of the parameters. Select the Parameter dialog box by pressing the $\overline{P}$ key. To set the value of a particular parameter, use the arrow keys to highlight the appropriate item. When the parameter is chosen, one may increment or decrement a digit (or units prefix) by pressing the $+$ and $-$ keys, respectively. Alternatively, one may enter the parameter value by positioning the cursor at the leftmost digit of the number and typing the desired value, followed by CR (Return). The K key permits keyboard entry as for the Axes and State boxes.

The program is preset with several default sets of parameters which may be accessed by pressing the D key. The default mode brings up a submenu from which one may choose one of the following attractors: EQ (equilibrium point), P1 (period-one periodic attractor), P2 (period-two periodic attractor), P4 (period-four periodic attractor), SC1 (Spiral Chua's chaotic attractor), P3 (period-three periodic attractor), SC2 (Spiral Chua's chaotic attractor), and DS (Double Scroll Chua's chaotic attractor). Use the arrow keys to move left or right to highlight the desired attractor, and press CR .

4.1.4. *View.* The (I_3, V_2, V_1) coordinate system may be viewed from various positions by applying the appropriate viewing transformation which is parametrized by ϕ and θ. We use ϕ to denote the angle of latitude (in degrees) measured from the North Pole, and θ to denote the angle of longitude. The View dialog box shows the current values of ϕ and θ and whether the eigenspaces and boundary planes are to be shown or not. See Fig. 10.

Press V to bring up the View dialog box. The viewing angle is entered by

```
φ   86°   ESPACES

θ   30°       ON
```

FIG. 10. View dialog box.

selecting the appropriate variable with the arrow cursor keys and incrementing, decrementing (by using the $+$ and $-$ key), or typing the value of each digit. The K key works as in the Axes dialog box.

Press T to toggle the equilibria, separating planes, and eigenspaces on and off.

4.2. *G bifurcation sequence*

In this tutorial, we study bifurcations and attractors in Chua's oscillator with L, R_0, C_2, G_a, G_b, E, and C_1 fixed at their default values (see Fig. 9) ; we vary G in the range $500~\mu S < G < 600~\mu S$.

Activate the Parameter dialog box by pressing P from the main menu.

Press D to bring up the defaults submenu.

Use the left arrow key to select EQ and press CR. Notice that G has been set to $510~\mu S$.

Press CR once more (or Esc) to deactivate the Parameter dialog box. We are now ready to run a simulation.

4.2.1. *Equilibrium point.* When G is small, the outer equilibrium points $\mathbf{P}_-$ and $\mathbf{P}_+$ of Chua's oscillator are *stable*, and the inner equilibrium point $\mathbf{0}$ is *unstable*.

Depending on the initial state of the circuit, the system remains at one outer equilibrium point or the other. Let us assume that we start at $\mathbf{P}_+$ in the D_1 region. This equilibrium point has one negative real eigenvalue and a complex pair with negative real parts. The action of the negative real eigenvalue is to squeeze trajectories down onto the complex eigenplane $E^c(\mathbf{P}_+)$ where they spiral towards the equilibrium point $\mathbf{P}_+$.

Choose the default state by pressing S , D , and CR (in that order) to activate the State dialog box, choose the default state, and deactivate the dialog box.

The R key initiates solution of the circuit equations from the chosen initial state. The integration routine calculates N timepoints with a fixed timestep h and returns the last calculated timepoint as the new state vector.

The number of timepoints N is fixed. The timestep h may be set by the user or chosen automatically (as $0.25/|\lambda_{max}|$ rounded down to the nearest multiple of 1, 2, or 5). You may change both N and h by pressing I to bring up the Integration dialog box.

The number of points in the time-series is entered by selecting N with the arrow cursor keys and incrementing, decrementing, or typing the value of each digit; similarly for h (note that the error is not controlled if the chosen stepsize is too large). The K key can also be used to enter values for N and h. Press T to toggle the automatic stepsize selection on and off.

Run the simulation by pressing R . This brings up the Eigenvalues message box on the right side of the screen which shows the eigenvalues for the outer (D_1, D_{-1}) and inner (D_0) regions. A typical Eigenvalues message box is shown in Fig. 11.

At the end of a run, the program draws the most recently evaluated time-series in the time window and extends the trajectory in phase space by N points.

With this set of parameters, the real parts of the eigenvalues of $\mathbf{P}_+$ and $\mathbf{P}_-$ are both negative. The outer equilibrium points are *stable*. Notice how the trajectory

```
┌─────────────────────────┐
│      EIGENVALUES        │
│                         │
│                         │
│      OUTER REGION       │
│     -2.3148D+04,        │
│     +6.0645D+02         │
│    +/-j0.192D+05        │
│                         │
│                         │
│      INNER REGION       │
│     +2.5358D+04,        │
│     -6.2222D+03         │
│    +/-j0.199D+05        │
└─────────────────────────┘
```

FIG. 11. Eigenvalues message box.

rapidly collapses onto the outer complex eigenplane $E^c(\mathbf{P}_+)$, along which it spirals towards $\mathbf{P}_+$.

4.2.2. *Hopf-like bifurcation.* As the conductance G is increased, the real part of the complex pair of eigenvalues changes sign and becomes positive. Correspondingly, the outer equilibrium points become unstable; this is called a *Hopf-like* bifurcation. The real eigenvalue of $\mathbf{P}_+$ remains negative so trajectories in the D_1 region converge towards the complex eigenplane $E^c(\mathbf{P}_+)$. However, they spiral *away* from the equilibrium point $\mathbf{P}_+$ along $E^c(\mathbf{P}_+)$ until they reach the dividing plane U_1 (defined by $V_1 = E$) and enter the D_0 region.

The equilibrium point at the origin in the D_0 region has a stable complex pair of eigenvalues and an unstable real eigenvalue. Trajectories which enter the D_0 region on the complex eigenplane $E^c(\mathbf{0})$ are attracted to the origin along this plane. Trajectories which enter D_0 from D_1 below or above the eigenplane either cross over to D_{-1} or are turned back towards D_1, respectively. For G sufficiently small, trajectories which spiral away from $\mathbf{P}_+$ along $E^c(\mathbf{P}_+)$ and enter D_0 *above* $E^c(\mathbf{0})$ are returned to D_1, producing a stable period-one *limit cycle*. See Fig. 12.

Press $\boxed{\text{P}}$ to select the parameters and use the arrow keys to highlight G. Use the $\boxed{+}$ key to increase the value of G to 520.1 μS. Press $\boxed{\text{CR}}$ to deactivate the dialog box.

Press $\boxed{\text{R}}$ to run the simulation. Notice that the real part of the complex pair of eigenvalues in the outer region is now very small but positive. The circuit undergoes a Hopf-like bifurcation (σ_1 passes through zero) close to this value of G. Increase the value of G to 530 μS and rerun the simulation. This time, the steady-state solution is a stable limit cycle (corresponding to the P1 default preset).

4.2.3. *Period-doubling.* As the conductance G is increased further, a period-doubling or *flip* bifurcation occurs. The limit cycle now closes on itself after encircling $\mathbf{P}_+$ *twice*; this is called a *period-two* cycle because a trajectory takes
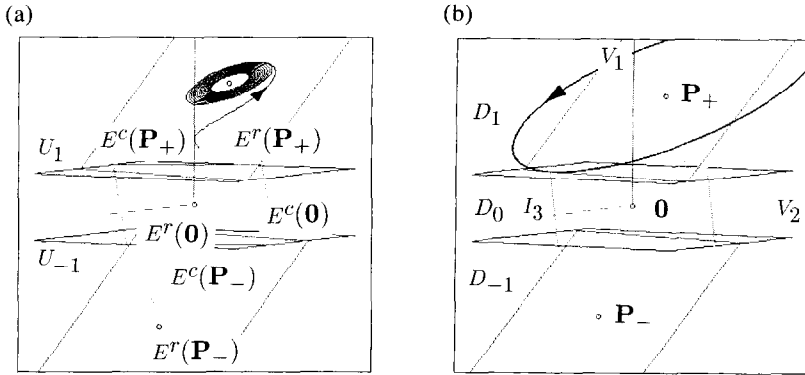
(a)

$E^c(\mathbf{P}_+)$ $E^r(\mathbf{P}_+)$

U_1

$E^r(0)$ $E^c(0)$

U_{-1}

$E^c(\mathbf{P}_-)$

$E^r(\mathbf{P}_-)$

(b)

V_1

D_1 $\mathbf{P}_+$

D_0 I_3 0 V_2

D_{-1}

$\mathbf{P}_-$

FIG. 12. Hopf-like bifurcation. (a) $L = 18$ mH, $R_0 = 12.5\ \Omega$, $C_2 = 100$ nF, $G = 510\ \mu$S, $G_a = -757.576\ \mu$S, $G_b = -409.09\ \mu$S, $E = 1$ V, $C_1 = 10$ nF. Since γ_1 is negative and the complex conjugate pair of eigenvalues in the outer region have negative real parts σ_1, a trajectory starting in D_1 approaches $\mathbf{P}_+$ asymptotically. The steady-state solution is the DC equilibrium point. (b) With $G = 520.1\ \mu$S and all other parameters as in (a), σ_1 is positive. The equilibrium point $\mathbf{P}_+$ is no longer stable. The steady-state solution is a limit cycle.

approximately twice the time to complete this closed orbit as to complete the preceding period-one orbit.

Increasing the conductance G still further produces a cascade of period-doubling bifurcations to *period-four*, *period-eight*, *period-sixteen*, and so on until an orbit of infinite period is reached, beyond which we have chaos. This is a Spiral Chua's *chaotic attractor*. See Fig. 13.

When $G = 541\ \mu$S (SC1), the Spiral Chua's attractor looks like a ribbon or band which is smoothly folded on itself; this folded band is the simplest type of strange attractor (11).

4.2.4. *Periodic windows.* Between the chaotic regions in the parameter space of Chua's oscillator, there exist ranges of the bifurcation parameter G over which stable periodic motion occurs. These regions of periodicity are called *periodic windows*.

Periodic windows of periods three and five are readily found in Chua's oscillator. These periodic limit cycles undergo period-doubling bifurcations to chaos as the conductance G is increased.

A period-three orbit, so-called because the trajectory encircles one of the outer equilibrium points three times before closing on itself, may be observed by selecting the P3 default parameter set. Note that there could be a long transient associated with the period-three orbit before steady-state is reached. Press R several times until the transient passes, then clear the windows with C and $\langle R \rangle$un the steady-state trajectory. See Fig. 14.

4.2.5. *Spiral Chua's attractor.* When $G = 550\ \mu$S, we obtain a Spiral Chua's strange attractor (SC2).

Rotate the attractor to $\phi = 90°$ and $\theta = 68°$ to get a view along the edge of the outer complex eigenplanes $E^c(\mathbf{P}_+)$ and $E^c(\mathbf{P}_-)$; notice how trajectories in the D_1 region are compressed towards the complex eigenplane $E^c(\mathbf{P}_+)$ along the direction
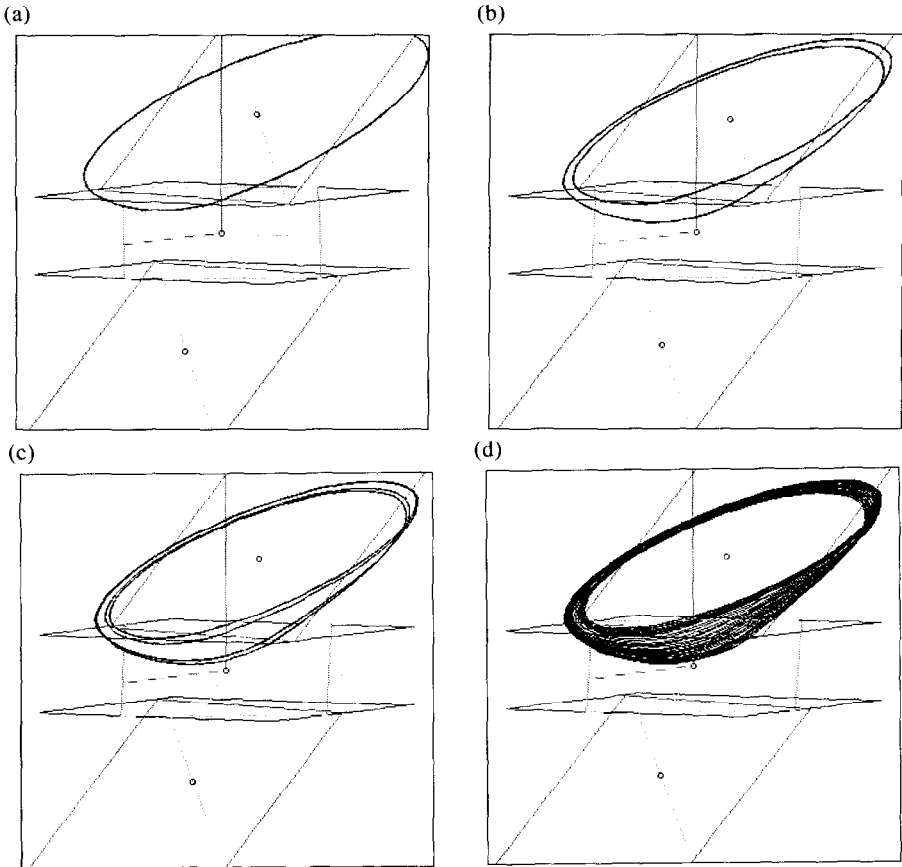
(a)

(b)

(c)

(d)

FIG. 13. G bifurcation sequence. $L = 18$ mH, $R_0 = 12.5$ Ω, $C_2 = 100$ nF, $G_a = -757.576$ μS, $G_b = -409.09$ μS, $E = 1$ V, $C_1 = 10$ nF. (a) $G = 530.0$ μS—period-one limit cycle, (b) $G = 537.0$ μS—period-two limit cycle, (c) $G = 539.0$ μS—period-four limit cycle, (d) $G = 541.0$ μS—Spiral Chua's chaotic attractor.

of the stable real eigenvector $E^r(\mathbf{P}_+)$ and that they spiral away from the equilibrium point $\mathbf{P}_+$ along $E^c(\mathbf{P}_+)$.

When a trajectory enters the D_0 region through U_1 from D_1, it is twisted around the unstable real eigenvector $E^r(\mathbf{0})$ and returned to D_1.

When the trajectory enters D_0 from D_1, it crosses U_1 *above* the eigenplane $E^c(\mathbf{0})$. The trajectory cannot cross through this eigenplane and therefore it must return to the D_1 region. Rotate to $\phi = 90°$, $\theta = 118°$ to see this more clearly. Figure 15 illustrates this.

4.2.6. *Double Scroll Chua's attractor.* Because we chose a nonlinear resistor with an odd-symmetric nonlinearity, every attractor which exists in the D_1 and D_0 regions has a counterpart (mirror image) in the D_{-1} and D_0 regions. As the coupling conductance G is increased further, the Spiral Chua's attractor "collides" with its image, reflected through the origin, and the two merge to form a single compound attractor called a Double Scroll Chua's strange attractor (2).
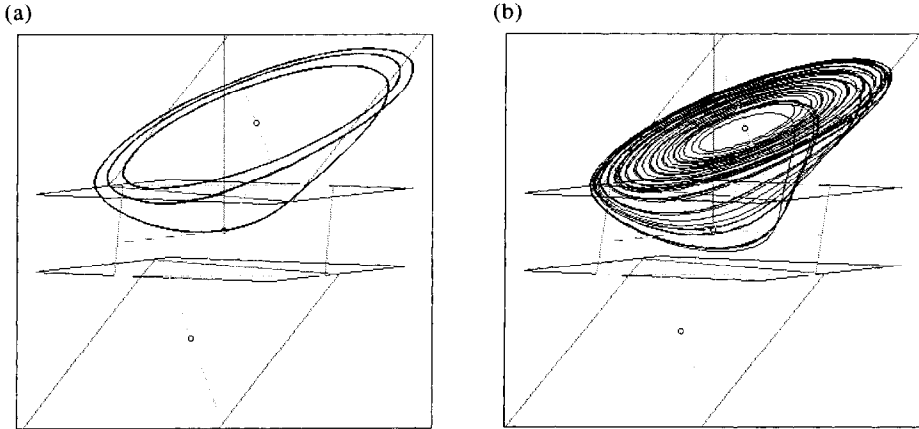
(a)

(b)

FIG. 14. G bifurcation sequence. $L = 18$ mH, $R_0 = 12.5$ Ω, $C_2 = 100$ nF, $G_a = -757.576$ μS, $G_b = -409.09$ μS, $E = 1$ V, $C_1 = 10$ nF. (a) $G = 542.5$ μS—period-three limit cycle, (b) $G = 550.0$ μS—Spiral Chua's chaotic attractor.
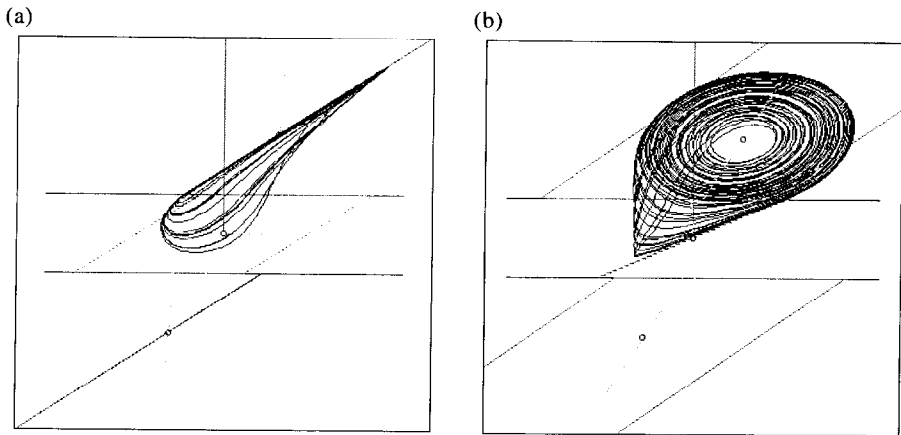
(a)

(b)

FIG. 15. Spiral Chua's attractor, viewed along the edges of $E^c(\mathbf{P}_+)$ and $E^c(\mathbf{0})$, respectively. (a) $\phi = 90°$, $\theta = 68°$, (b) $\phi = 90°$, $\theta = 118°$.

Run the simulation with the DS default parameters.

Set the viewing coordinates to $\phi = 90°$, $\theta = 66°$ to view the attractor along the edge of the outer complex eigenplanes $E^c(\mathbf{P}_+)$ and $E^c(\mathbf{P}_-)$. Upon entering the D_1 region from D_0, the trajectory collapses onto $E^c(\mathbf{P}_+)$ and spirals away from $\mathbf{P}_+$ along this plane.

Set the view to $\phi = 90°$, $\theta = 118°$ to see the attractor along the edge of the complex eigenplane $E^c(\mathbf{0})$ in the inner region. Notice once more that when the trajectory crosses U_1 into D_0 above $E^c(\mathbf{0})$, it must remain above $E^c(\mathbf{0})$ and so returns to D_1. Similarly, if the trajectory crosses U_1 below $E^c(\mathbf{0})$, it must remain below $E^c(\mathbf{0})$ and therefore crosses over to the D_{-1} region. Thus, $E^c(\mathbf{0})$ presents a
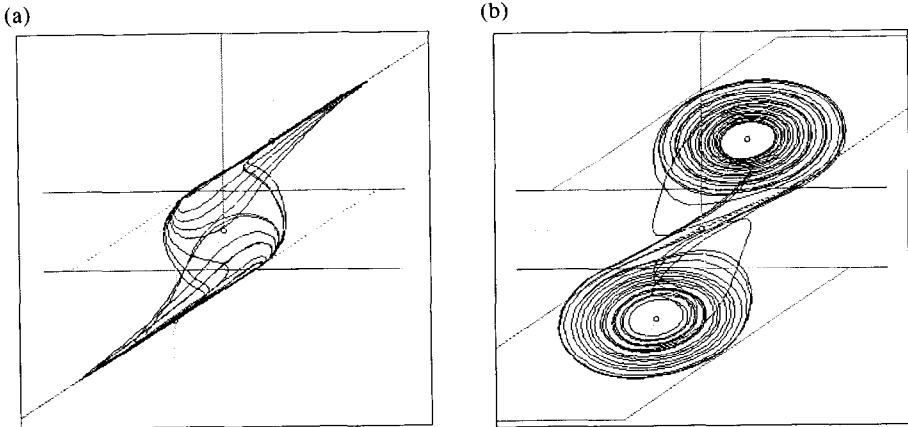
(a)   (b)

FIG. 16. Double Scroll Chua's attractor, viewed along the edges of $E^c(\mathbf{P}_+)$ and $E^c(\mathbf{0})$, respectively. (a) $\phi = 90°$, $\theta = 66°$, (b) $\phi = 90°$, $\theta = 118°$.

knife-edge to the trajectory as it crosses U_1 into the D_0 region, forcing it back towards D_1 or across D_0 to D_{-1}. This is illustrated in Fig. 16.

4.2.7. *Boundary crisis.* As G is increased further, the attractor decreases in size until a *boundary crisis* (2) occurs, beyond which all trajectories of the circuit eventually become unbounded and the simulation fails.

4.3. *Alternative bifurcation sequence*

Notice that varying G in this way causes the size of the attractors to change: the period-one orbit is large, period-two is smaller, the Spiral Chua's attractor is smaller still, and the Double Scroll Chua's attractor shrinks considerably before it dies. This shrinking is due to the equilibrium points $\mathbf{P}_+$ and $\mathbf{P}_-$ moving closer towards the origin as G is increased. Compare the distance of $\mathbf{P}_+$ from the origin for the EQ and DS parameter sets.

An alternative way to view a bifurcation sequence is by adjusting C_1. Fix the value of G at 555.556 μS and vary C_1. The full range of dynamical behaviors from equilibrium through Hopf and period-doubling bifurcations, periodic windows, Spiral Chua's chaotic attractors and Double Scroll Chua's chaotic attractors can be observed as C_1 is reduced from 11.0 nF to 7.5 nF. Unlike the G bifurcation sequence, the size of the Double Scroll Chua's attractor remains almost constant in the C_1 bifurcation sequence because the *positions* of the equilibrium points are independent of C_1. See Fig. 17.

4.4. *Saving your work*

There are several ways in which the data generated by ABC can be stored. The calculated trajectory can be stored in a buffer by means of the $\langle$B$\rangle$uffer submenu or in a data file on disk by means of the $\langle$F$\rangle$ile submenu. In addition, the parameters, current state vector, viewing parameters, integration timestep and other data can be stored in an options file on disk using the $\langle$F$\rangle$ile submenu.
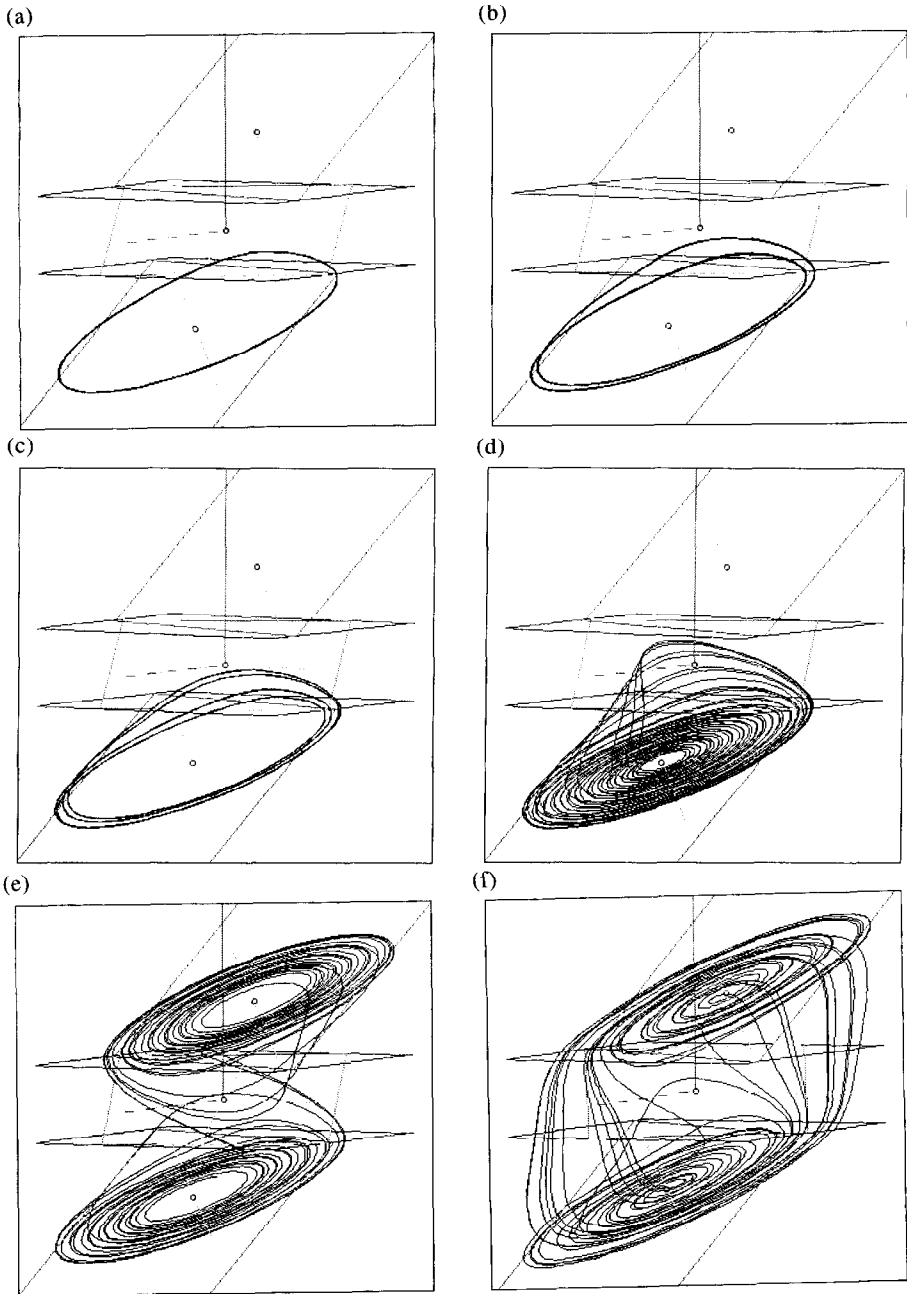
(a)

(b)

(c)

(d)

(e)

(f)

FIG. 17. C_1 bifurcation sequence. $L = 18$ mH, $R_0 = 12.5\ \Omega$, $C_2 = 100$ nF, $G = 555.556\ \mu S$, $G_a = -757.576\ \mu S$, $G_b = -409.09\ \mu S$, $E = 1$ V. (a) $C_1 = 10.75$ nF—period-one limit cycle, (b) $C_1 = 10.5$ nF—period-two limit cycle, (c) $C_1 = 10.4$ nF—period-four limit cycle, (d) $C_1 = 10.1$ nF—Spiral Chua's chaotic attractor, (e) $C_1 = 10.0$ nF—Double Scroll Chua's chaotic attractor, (f) $C_1 = 8.0$ nF—Double Scroll Chua's chaotic attractor.

STATE			
I3	+	948.223	uA
V2	+	220.107	mV
V1	+	169.098	mV

STATE			
I3	-	948.223	uA
V2	-	220.107	mV
V1	-	169.098	mV

FIG. 18. Initial states which produce Spiral Chua's chaotic attractors. (a) This inital state produces the upper attractor in Fig. 19(a). (b) This inital state produces the lower attractor in Fig. 19(a). Note that the attractors are images of each other, reflected through the origin.

4.4.1. *Buffer submenu.* The trajectory generated by the ⟨R⟩un command can be stored in a buffer whose contents can be displayed alongside new trajectories generated by the ⟨R⟩un command. This is useful in studying bifurcation behavior by storing the attractor for one parameter set in the buffer while generating the attractor for another parameter set and displaying both trajectories simultaneously. It is also useful for displaying co-existing attractors, where there are several attractors for the same parameter set. Which one of the attractors the trajectory will settle to depends on the initial values for the state vector.

The Buffer submenu consist of three choices, ⟨C⟩opy to Buffer, ⟨S⟩how Buffer, and ⟨H⟩ide Buffer. Pressing the | C key copies the current trajectory into the Buffer. Pressing the | S key will show the trajectory in the Buffer alongside the generated trajectory each time ⟨R⟩un is executed from the main menu. The newly-generated current trajectory is shown in white and the trajectory in the Buffer is shown in gray. If the H key is pressed, the program will not show the trajectory in the Buffer.

As an example, consider the Spiral Chua's attractor. As mentioned before, an identical twin of the chaotic attractor is located symmetrically with respect to the origin. To display both of them, first select the default parameters by pressing P
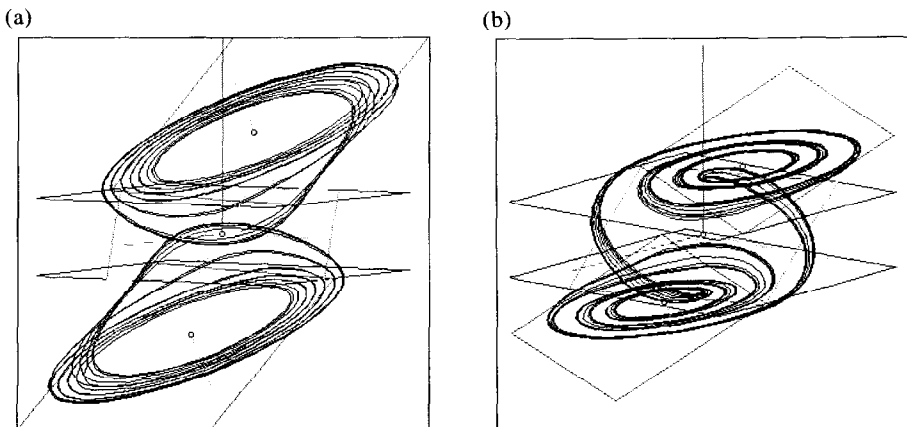
(a)

(b)

FIG. 19. (a) Two Spiral Chua's attractors displayed simultaneously by using the ⟨B⟩uffer commands. (b) Attractors produced from the database using the ⟨F⟩ile commands: CO3A.OPT and CO3B.OPT.

```
┌─────────────────────┐
│   OPTIONS FILE      │
│    TEST.OPT         │
│  DATA FILE (C)      │
│    TEST.DAT         │
└─────────────────────┘
```
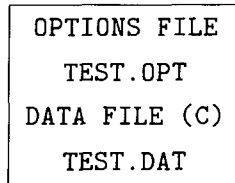
FIG. 20. File message box.

from the main menu and then the D key. Select the parameter set SC2. Press
 Esc to return to the main menu. Press S and enter the states shown in Fig.
18(a).

Return to the main menu and press R to start the simulation. Then press B
to bring up the Buffer submenu and C | to save the trajectory to the Buffer. Then
press S to show the Buffer trajectory. Next enter the states shown in Fig. 18(b).

Note that this is just the state we entered earlier, but reflected through the origin.
Now press R | to see both attractors simultaneously.

4.4.2. *File submenu*. Instead of typing in a new set of parameters each time one
runs the program, one may load the values from an options file by choosing the
⟨F⟩ile option from the main menu.

Pressing the| F button brings up the ⟨F⟩ile submenu.

The ⟨S⟩ave file option prompts the user for the names of files in which to save
options from a simulation. An options file has a .OPT extension and the user enters
the filename without the extension.

The ⟨L⟩oad file option allows the user to load parameters and other options
from a file. The user enters the file name as in the ⟨S⟩ave file option.

The trajectory generated by the program can be saved in a data file in ASCII
format with the parameters of the simulation as a header. Data files have a .DAT
extension and the user enters the filename without the extension. The ⟨O⟩pen data
file option opens a data file for storage and writes the parameters and the initial
state to the file. Every time the R key is pressed from the main menu, the data
of the generated trajectory will be appended to the data file. The data file is closed
when the ⟨C⟩lose data file option is selected, parameters or states are changed, or
the program is exited.

The File message box shows the most recently used file names for the options
file and the data name. The status of the data file is also shown in the File box,
where an (O) next to the words DATA FILE indicates that the data file is open
and a (C) indicates that it is closed. See Fig. 20.

4.4.3. *Options file on disk*. Appendix B contains a list of the options files supplied
in the ABC database and the corresponding behaviors in Chua's oscillator. Also
included with the database is an ASCII file called PARAM.TXT which contains a
description of each options file: the parameters, the initial conditions, the eig-
envalues of the three regions and the associated behavior are given. Associated
with each entry is a code. For example, the entry with code HO1, listed under
"miscellaneous pheonomena", corresponds to the options file HO1.OPT. Loading
this file and hitting ⟨R⟩un will produce the corresponding trajectory, in this case
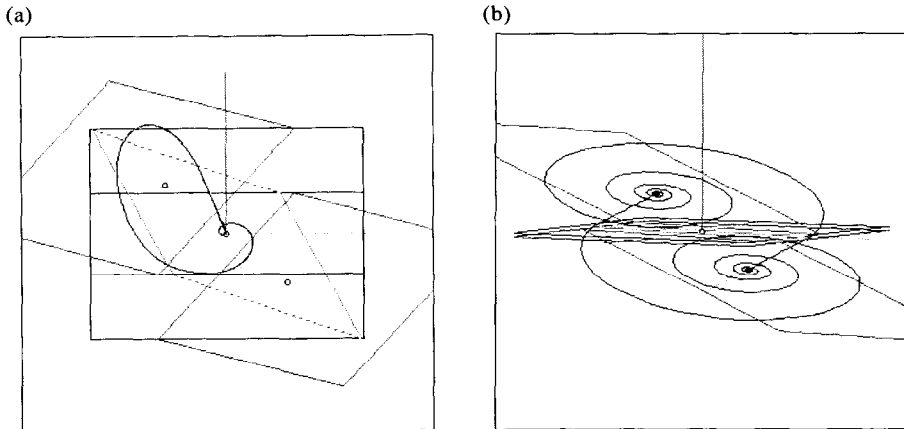a homoclinic trajectory, shown in Fig. 21(a).

(a)

(b)

FIG. 21. (a) Homoclinic orbit produced by HO1.OPT connects **0** to itself in forward and reverse time. (b) Heteroclinic trajectories linking $\mathbf{P}_+$ and $\mathbf{P}_-$. The corresponding parameters and initial conditions are stored in files HE1A.OPT and HE1B.OPT.

4.4.4. Hardcopy. The graphics shell command in DOS 5.0 allows one to dump the PC's screen to a printer by pressing the | Print Screen | key.

For example, if a LaserJetII printer is connected to your computer, add the following line to your AUTOEXEC.BAT file: graphics laserjetii. See your DOS manual for further details.

4.5. *Quit*

The program is exited by pressing Q |. If the user confirms by typing Y | and CR |, then the program is halted and exited gracefully.

4.6. *Future versions of ABC*

ABC is maintained by the author and future versions of this program will be available from him. The program may be obtained by anonymous ftp from the directory pub/ABC on vdp.ucd.ie (IP address 137.43.24.130).

Acknowledgements

References

(1) L. O. Chua, "Global unfolding of Chua's circuit", *IEICE Trans. Fund. (Special Issue on Chaos, Neural Networks, and Numerics)*, Vol. E76-A, pp. 704–734, May 1993.
(2) L. O. Chua, M. Komuro and T. Matsumoto, "The Double-Scroll family, parts I and II", *IEEE Trans. Circuits & Syst.*, Vol. CAS-33, pp. 1073–1118, 1986.

(3) L. O. Chua, C. A. Desoer and E. S. Kuh, "Linear and Nonlinear Circuits", McGraw-Hill, New York, 1987.

(4) M. P. Kennedy, "Robust op amp realization of Chua's circuit", *Frequenz*, Vol. 46, pp. 66–80, March–April 1992.

(5) M. P. Kennedy, "Three steps to chaos part I: Evolution", *IEEE Trans. Circuits & Syst. (Part I)*, Vol. 40, pp. 640–656, 1993.

(6) M. P. Kennedy, "Three steps to chaos part II: A Chua's circuit primer", *IEEE Trans. Circuits & Syst. (Part I)*, Vol. 40, pp. 657–674, 1993.

(7) R. N. Madan (Ed.), "Chua's Circuit: A Paradigm for Chaos", World Scientific, Singapore, 1993.

(8) C. Wu and N. F. Rul'kov, "Studying chaos near one-dimensional maps: A tutorial", *IEEE Trans. CAS (Special Issue on Chaos in Nonlinear Circuits)*, Vol. CAS-40, pp. 707–721, October 1993.

(9) I. N. Bronshtein and K. A. Semendyayev, "Handbook of Mathematics", Van Nostrand Reinhold, New York, 1985.

(10) M. P. Kennedy, C. W. Wu, S. Pau and J. Tow, "Digital signal processor-based investigation of Chua's circuit family", *J. Circuits Syst. Comput.*, Vol. 3, pp. 269–292, June 1993.

(11) J. M. T. Thompson and H. B. Stewart, "Nonlinear Dynamics and Chaos", Wiley, New York, 1986.

Appendix A. Notation quick reference

State variables

I3	Current in inductor L (and R_0)	BRIGHTRED
V2	Voltage across capacitor C_2	BRIGHTGREEN
V1	Voltage across capacitor C_1	BRIGHTBLUE

Phase space geometry

D_1	Outer region ($V_1 > E$)	
P_+	Equilibrium point in the D_1 region	WHITE
$E^r(P_+)$	Eigenspace spanned by the real eigenvector of P_+	BRIGHTMAGENTA
$E^c(P_+)$	Eigenspace spanned by the complex eigenvectors of P_+	MAGENTA
U_1	Boundary between the D_1 and D_0 regions ($V_1 = E$)	BLUE
D_0	Inner region ($-E < V_1 < E$)	
$\mathbf{0}$	Equilibrium point at the origin (in the D_1 region)	WHITE
$E^r(\mathbf{0})$	Eigenspace spanned by the real eigenvector of $\mathbf{0}$	BRIGHTCYAN
$E^c(\mathbf{0})$	Eigenspace spanned by the complex eigenvectors of $\mathbf{0}$	CYAN
U_{-1}	Boundary between the D_0 and D_{-1} regions ($V_1 = -E$)	BLUE
D_{-1}	Outer region ($V_1 < -E$)	
P_-	Equilibrium point in the D_{-1} region	WHITE
$E^r(P_-)$	Eigenspace spanned by the real eigenvector of P_-	BRIGHTMAGENTA
$E^c(P_-)$	Eigenspace spanned by the complex eigenvectors of P_-	MAGENTA

Currently generated trajectory   WHITE
Trajectory stored in Buffer   GRAY

Appendix B. Database of bifurcation phenomena and attractors

ABC is supplied with a database of options files containing parameter sets for Chua's oscillator which produce a variety of dynamical phenomena. Also included are initial conditions for the attractors, recommended window bounds for a two-dimensional projection of the state space, integration stepsizes h, and eigenvalues (computed for the circuit parameters).

Figure 22 shows typical trajectories for some representative files in the database.

Routes to chaos

Period-doubling route to chaos (bifurcation parameter C_1)
PD1	period-1 attractor (period-doubling route)
PD2	period-2 attractor (period-doubling route)
PD3	period-4 attractor (period-doubling route)
PD4	period-8 attractor (period-doubling route)
PD5	Spiral Chua's attractor (period-doubling route)
PD6	Double Scroll Chua's attractor (period-doubling route)

Intermittency route to chaos (bifurcation parameter L)
I1	periodic attractor (intermittency route)
I2	periodic attractor (intermittency route)
I3	chaotic attractor (intermittency route)
I4	chaotic attractor (intermittency route)
I5	chaotic attractor (intermittency route)
I6	chaotic attractor (intermittency route)

Torus breakdown route to chaos (bifurcation parameter C_1)
TB1	periodic attractor (torus breakdown route)
TB2	periodic attractor (torus breakdown route)
TB3	torus attractor (torus breakdown route)
TB4	periodic attractor (torus breakdown route)
TB5	periodic attractor (torus breakdown route)
TB6	chaotic attractor (torus breakdown route)

Period adding (bifurcation parameter R)
PA1	period-2 : 2 attractor (period adding)
PA2	period-3 : 3 attractor (period adding)
PA3	period-4 : 4 attractor (period adding)
PA4	period-5 : 5 attractor (period adding)
PA5	period-6 : 6 attractor (period adding)

Symmetry breaking (bifurcation parameter C_2)
SB1	odd-symmetric periodic attractor (symmetry breaking)
SB2 (a–b)	two asymmetric periodic attractors (symmetry breaking)
SB3	odd-symmetric periodic attractor (symmetry breaking)

Gallery of attractors

Periodic attractors
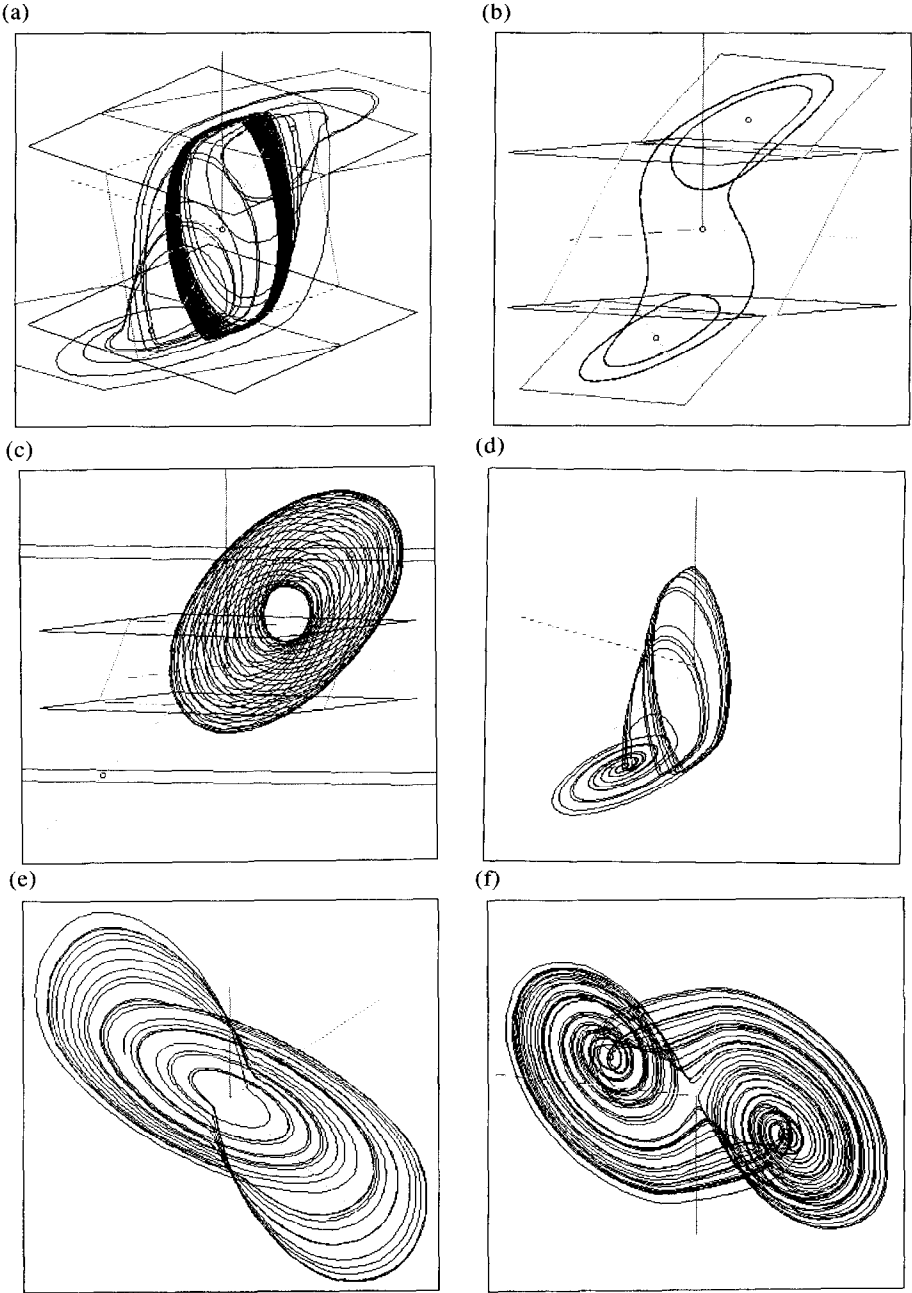|	
GP1	periodic attractor (gallery of attractors)
GP2	periodic attractor (gallery of attractors)

(a)

(b)

(c)

(d)

(e)

(f)

FIG. 22. Selection of attractors from the ABC database. (a) I3—intermittency, (b) SB2A—symmetry-breaking, (c) GQ3—torus (quasiperiodic) attractor, (d) GC6—chaotic attractor (eigenspaces switched off), (e) GC14—chaotic attractor, (f) GC18—Double Hook chaotic attractor.

Quasiperiodic attractors
GQ1   torus attractor (gallery of attractors)
GQ2   torus attractor (gallery of attractors)
GQ3   torus attractor (gallery of attractors)
GQ4   torus attractor (gallery of attractors)
Chaotic attractors
GC1   chaotic attractor (gallery of attractors)
GC2   chaotic attractor (gallery of attractors)
GC3   chaotic attractor (gallery of attractors)
GC4   chaotic attractor (gallery of attractors)
GC5   chaotic attractor (gallery of attractors)
GC6   chaotic attractor (gallery of attractors)
GC7   chaotic attractor (gallery of attractors)
GC8   chaotic attractor (gallery of attractors)
GC9   chaotic attractor (gallery of attractors)
GC10   chaotic attractor (gallery of attractors)
GC11   chaotic attractor (gallery of attractors)
GC12   chaotic attractor (gallery of attractors)
GC13   chaotic attractor (gallery of attractors)
GC14   chaotic attractor (gallery of attractors)
GC15   chaotic attractor (gallery of attractors)
GC16   chaotic attractor (gallery of attractors)
GC17   chaotic attractor (gallery of attractors)
GC18   Double Hook (gallery of attractors)
GC19   chaotic attractor (gallery of attractors)
GC20   chaotic attractor (gallery of attractors)
GC21   chaotic attractor (gallery of attractors)

Coexistence of attractors
CO1 (a–b)   periodic attractor + chaotic attractor (coexistence)
CO2 (a–c)   point attractor + periodic attractor + chaotic attractor (coexistence)
CO3 (a–b)   two chaotic attractors (coexistence)
CO4 (a–c)   three chaotic attractors (coexistence)
CO5 (a–f)   five attractors : two point attractors + three periodic attractors (coexistence)

Miscellaneous phenomena
S1   semiperiodic behavior
P1   transient behavior (preturbulence)
P2   periodic attractor after transient has died out (preturbulence)
HE1 (a–b)   heteroclinic orbit
HO1   homoclinic orbit
HO2   homoclinic orbit
HO3   homoclinic orbit
HO4   homoclinic orbit
HO5   homoclinic orbit

Other bifurcation sequences
AR1   periodic attractor (bifurcation parameter L)
AR2   strange attractor (bifurcation parameter L)
BR1   strange attractor (bifurcation parameter L)
BR2   strange attractor (bifurcation parameter L)
BR3   strange attractor (bifurcation parameter L)

BR4   strange attractor (bifurcation parameter L)
CR1   strange attractor (bifurcation parameter C_2)
CR2   strange attractor (bifurcation parameter C_2)
CR3   strange attractor (bifurcation parameter R)
CR4   strange attractor (bifurcation parameter R)
CR5   strange attractor (bifurcation parameter R)
CR6   period-6 attractor (bifurcation parameter R)
CR7   strange attractor (bifurcation parameter R)
CR8   period-8 attractor (bifurcation parameter R)
CR9   period-4 attractor (bifurcation parameter R)
CR10   period-2 attractor (bifurcation parameter R)
CR11   period-1 attractor (bifurcation parameter R)
DR1   strange attractor (bifurcation parameter R_0)
DR2   period-3 attractor (bifurcation parameter R_0)
DR3   period-2 attractor (bifurcation parameter R_0)
DR4   period-1 attractor (bifurcation parameter R_0)
DR5   strange attractor (bifurcation parameter R_0)